A mesoporous cationic metal-organic framework with high density of positive charge for enhanced removal of dichromate from water

Yu-Huang Zou,[ab] Jun Liang,[b] Chang He,[b] Yuan-Biao Huang,[*bc] and Rong Cao[abc]

[a]**Department of Chemistry, School of Chemistry and Materials Science, University of Science and technology of China, Anhui, Hefei 230000, P. R. China;**

[b]**State Key Laboratory of Structural Chemistry, Fujian Institute of Research on the Structure of Matter, Chinese Academy of Sciences, Fujian, Fuzhou 350002, P. R. China;**

[c]**University of the Chinese Academy of Sciences, Beijing 100049, P. R. China**

1.1Materials and characterization.

2-(Imidazol-1-yl)terephthalic acid was synthesized according to previous report.[1,2] MOFs including MIL-101[3] and (Cl^-)Etim-UiO-66[1,2] were synthesized and characterized according to references and activated before catalysis tests. All solvents and reagents were commercially available and used without further purification. N_2 sorption isotherms for MOFs were measured by using a Micrometrics ASAP 2460 instrument at 77 K. Before the measurement, the samples were evacuated and activated at 423 K in vacuum for 12 hours. Powder X-ray diffraction patterns (PXRD) were recorded on a Rigaku Dmax 2500 diffractometer equipped with Cu-Kα radiation (λ= 1.54056 Å) over the 2θ range of 4-40° with a scan speed of 3° min^{-1} at room temperature. Infrared (IR) spectra were recorded using KBr pellets on a PerkinElmer Spectrum One in the range of 400-4000 cm^{-1}. The ^1H NMR was performed at AVANCE III Bruker Biospin spectrometer, operating at 400 MHz. The morphologies of MOFs were studied using a FEIT 20 transmission electron microscope (TEM) working at 200 kV and scanning electron microscope (SEM) working at 10 KV.

1.2 Synthesis of (Cl^-)Etim-H_2BDC and FJI-C11

Synthesis of (Cl^-)Etim-H_2BDC: The ligand (Cl^-)Etim-H_2BDC was synthesized according to the literature.[1,2]

Synthesis of (Cl^-)Etim-UiO-66 and MIL-101: These MOFs were synthesized according to the literature.[1-3]

Synthesis of FJI-C11: [(Cl^-)Etim-H_2BDC] (34 mg, 0.1 mmol) and $CrCl_3\cdot 6H_2O$ (27 mg, 0.1 mmol) in 0.5 mL mixed solvent (H_2O/EtOH =1:1) were ultrasonically dissolved in a 10 mL Teflon-lined bomb. The mixture was heated in 180 ℃ oven for 12 h. After cooling down to room temperature, green precipitate was harvested by filtration. To activate FJI-C11, the obtained sample was dispersed in water and sealed at 80 ℃ for 6 h, repeat twice. Then FJI-C11 was dispersed in ethanol and activated at 80 ℃ for 10 h. After removal of ethanol by filtration, the sample was dried in vacuum for 12 h at 150 ℃.

1.3 Details of $Cr_2O_7^{2-}$ adsorption test

Exchange Kinetics Studies. The anion exchange experiment was performed by mixing the dried FJI-C11 (10 mg) with 20 ml 50 ppm dichromate solution and stirring under ambient conditions. During the experiment, 2 ml solution of the mixture was withdrawn and filtered with a 0.22 μm membrane filter on a regular basis. The remaining $Cr_2O_7^{2-}$ after adsorption in the aqueous was monitored by UV/Vis absorption spectroscopic at 350 nm.

The pseudo second-order equation can be expressed as non-linear forms by Eq. (1):

$$Q_t = \frac{k_2 Q_e^2 t}{1 + k_2 Q_e t} \qquad (1)$$

Where Q_e and Q_t are the amount of adsorbate (mg/g) onto adsorbent at the equilibrium and time t (min), respectively. Based on the pseudo second-order kinetic model, the initial adsorption rate h ($mg\cdot g^{-1}\cdot min^{-1}$) and half-adsorption time $t_{1/2}$ (min) were calculated according to the following equation:

$$h = k_2 Q_e^2 \qquad (2)$$

$$t_{1/2} = \frac{1}{k_2 Q_e} \qquad (3)$$

Sorption isotherm experiments. The $Cr_2O_7^{2-}$ adsorption isotherm experiments for FJI-C11 were performed by changing the initial $Cr_2O_7^{2-}$ concentration from 50 to 400 ppm. During the experiment, 10 mg of FJI-C11 was mixed with 20 mL of aqueous solution which contained different concentration of $Cr_2O_7^{2-}$. The mixture was stirred for 24 h to make sure to reach equilibrium and separated using 0.22 μm membrane filter. The remained concentrations of $Cr_2O_7^{2-}$ were determined by UV/Vis. The equilibrium adsorption capacity Q_e was calculated according to Eq. (4)

$$Q_e = \frac{(C_0 - C_e)V}{m} \qquad (4)$$

Where C_0 and C_e (mg/L) were the initial and final concentrations of $Cr_2O_7^{2-}$, respectively. V (L) was the volume of the solution, and m (g) was the mass of sorbent.

Recyclability studies. The activated FJI-C11 mixed with 300 ppm dichromate solution in the case of agitation for 24h. Then, the samples were centrifuged, wash with water, and immersed in the same volume solution which contained a 200-fold molar excess of chloride for 24h, repeated for 3 times. After collected by centrifugation, washed with water and ethanol and dried in vacuum for 12 h at 150 ℃, the sample was performed adsorption tests as mentioned above.

Selectivity performance studies. To investigate the selectivity performance of FJI-C11, n-fold (n = 0, 3, 6, 9, 12) molar excess of disturbing ions including F^-, Cl^-, Br^-, and NO^{3-} were added into a 20 mL solution of 50 ppm dichromate. Then, the selectivity adsorption tests were carried as same the adsorption isotherm experiments.

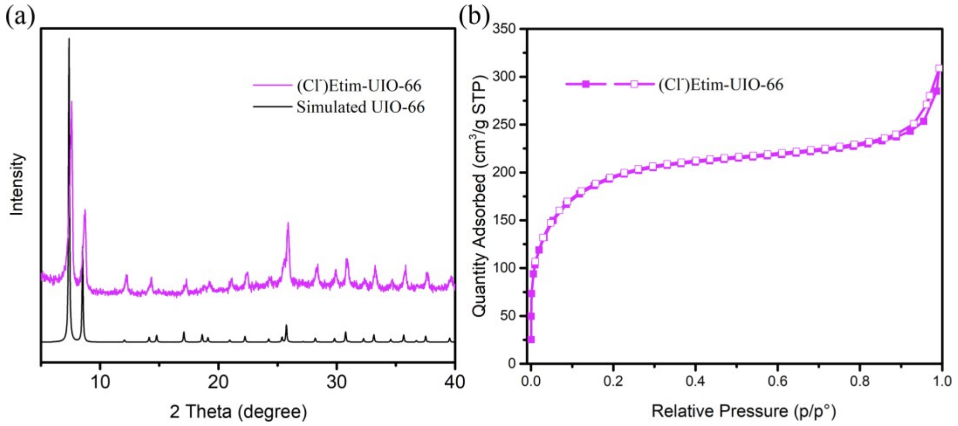

Figure. S1 PXRD patterns (a) and N_2 sorption curves (b) of (Cl$^-$)Etim-UiO-66.

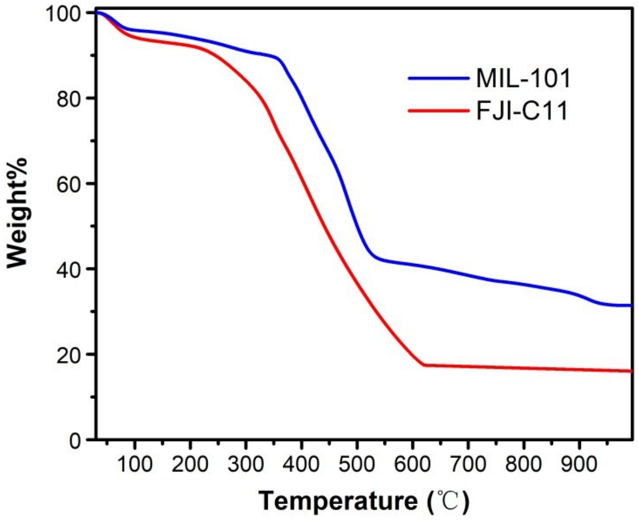

Figure. S2 TGA curves of MIL-101 and FJI-C11.

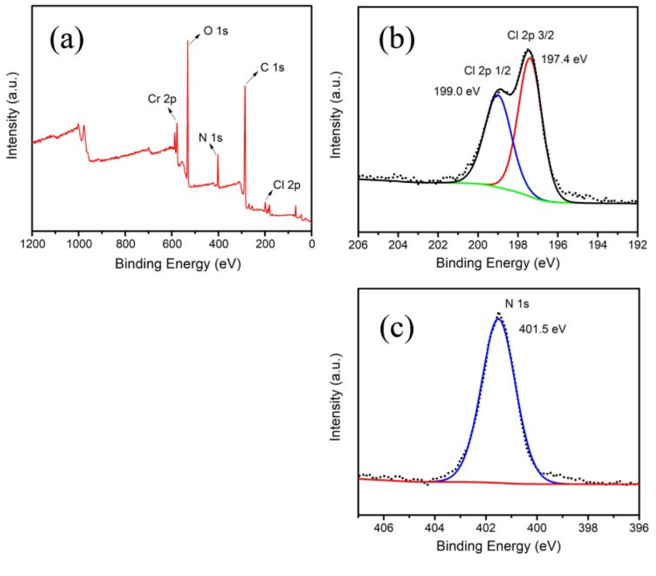

Figure. S3 XPS survey spectra (a), Cl 2p spectra (b) and N 1s spectra (c) of FJI-C11.

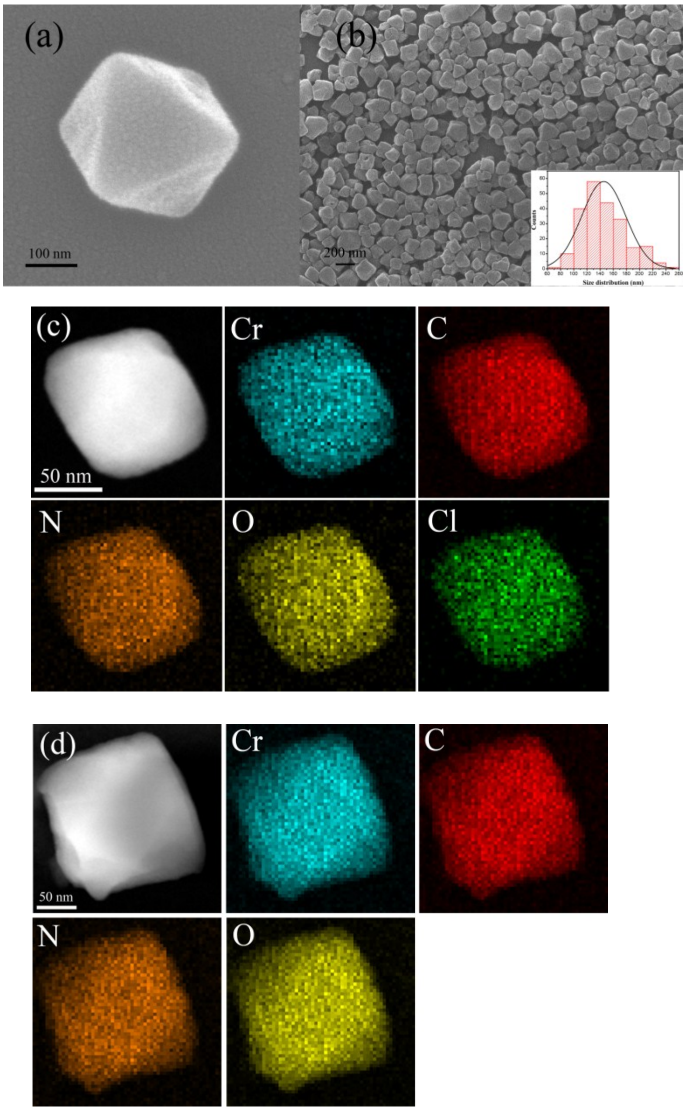

Figure. S4 The SEM images of different scale bars, 100 nm (a), 200 nm (b) and size distribution (insert) of FJI-C11. Typical STEM image of FJI-C11 (c) and FJI-C11 after adsorption (d) and the corresponding EDX elemental mapping images (Cr, C, N, O, and Cl).

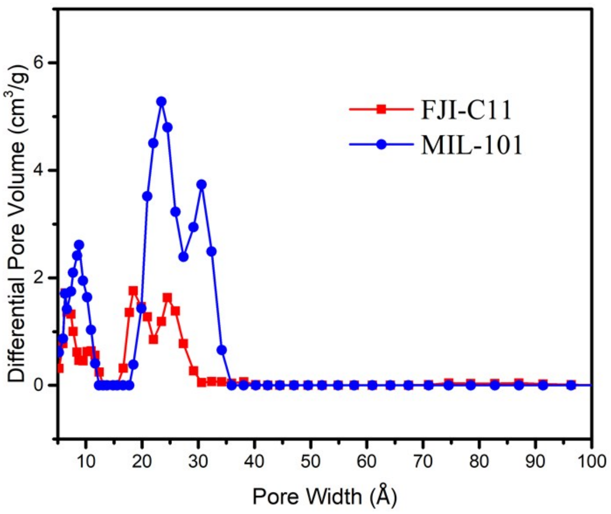

Figure. S5 Pore size distribution of MIL-101 and FJI-C11.

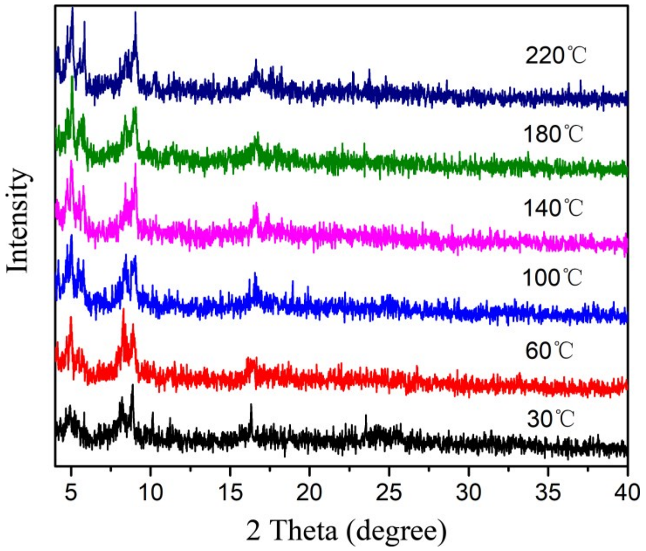

Figure. S6 Temperature-variable PXRD data for FJI-C11.

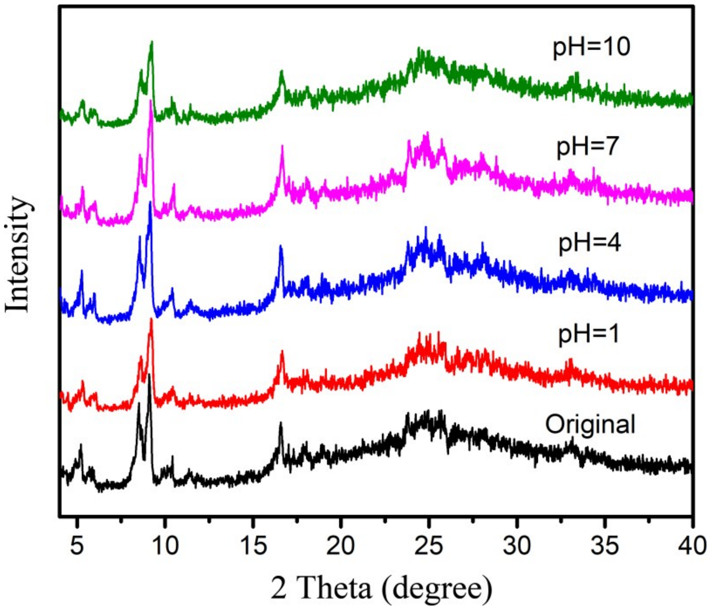

Figure. S7 PXRD data for FJI-C11 after soaking in different pH solution.

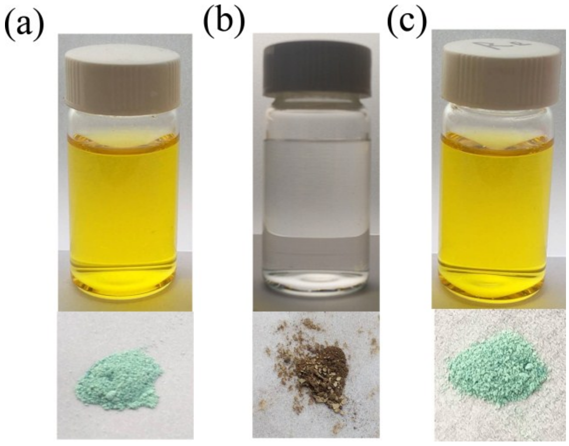

Figure. S8 (a) 300ppm dichromate solution and FJI-C11; (b) Chloride solution and FJI-C11 after adsorbing $Cr_2O_7^{2-}$; (c) Chloride solution and FJI-C11 after releasing $Cr_2O_7^{2-}$.

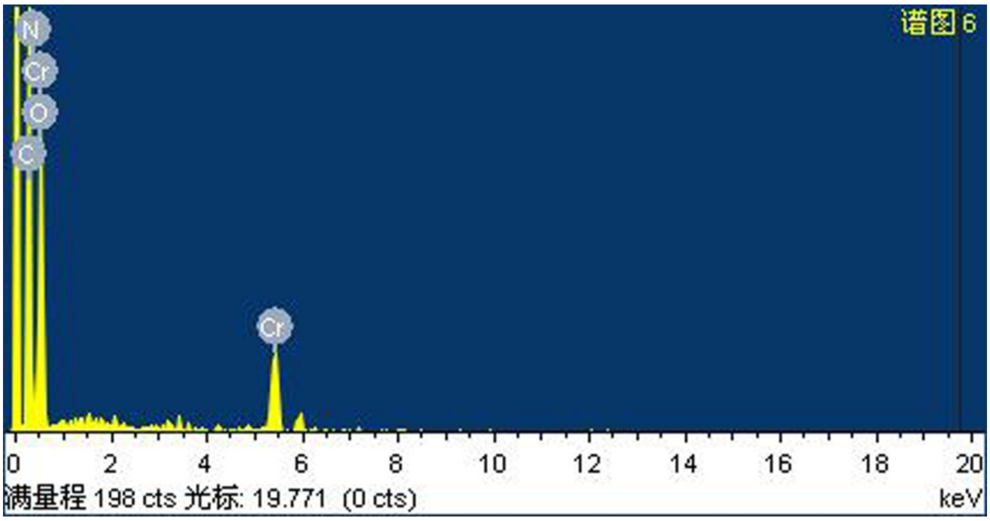

Figure. S9 EDS images of FJI-C11 after adsorption.

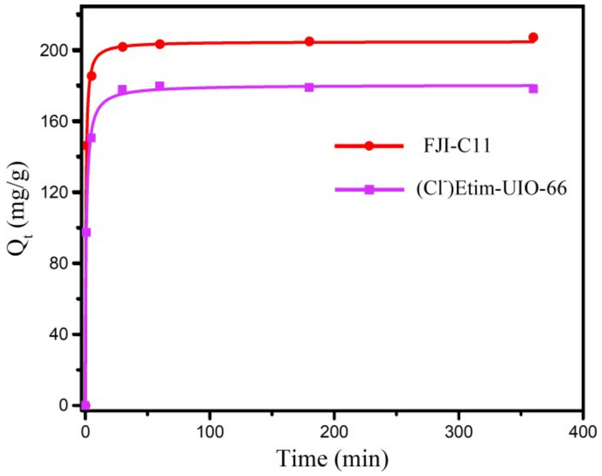

Figure. S10 Effect of time on the adsorption of $Cr_2O_7^{2-}$ by 10 mg adsorbents with 20 mL dichromate aqueous solution of 150 ppm.

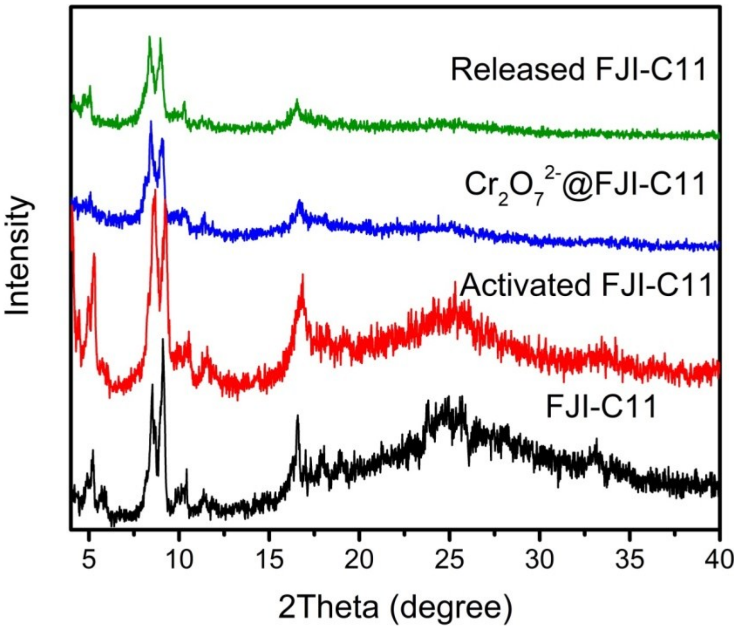

Figure. S11 PXRD data for FJI-C11 after adsorption and released.

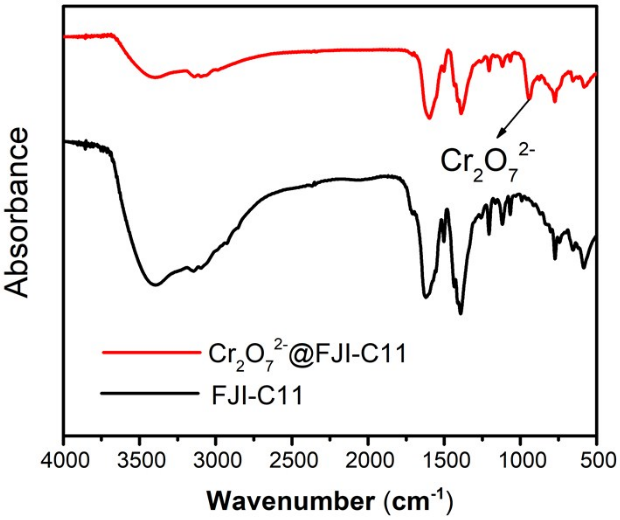

Figure. S12 FT-IR spectra of FJI-C11 and FJI-C11 after adsorption.

Table S1. ICP and element analysis of FJI-C11.

	Cr	C	O	N
ICP	11.94%			
Element analysis		37.63%	42.77%	6%

Table S2. BET surface area, pore volume and pore size of MIL-101, FJI-C11 and (Cl^-)Etim-UiO-66.

	BET surface area ($m^2\cdot g$)	Pore volume ($cm^3\cdot g^{-1}$)	Pore size (Å)
MIL-101	2961	1.447	8.7 / 23.6 / 30.5
FJI-C11	1201	0.971	6.2 / 18.5 / 24.6
(Cl^-)Etim-UiO-66	640	0.117	6.3 / 10.2 / 18.4

Table S3. Kinetic constants of MIL-101, FJI-C11 and (Cl^-)Etim-UiO-66 in dichromate solution with different concentration .

	concentration of dichromate solution (ppm)	initial adsorption rate h ($mg\cdot g^{-1}\cdot min^{-1}$)	half-adsorption time $t_{1/2}$ (min)	pseudo-second-order kinetic constant k_2 ($g\cdot mg^{-1}\cdot min^{-1}$)
MIL-101	50	0.0773	88.6	0.00165
FJI-C11	50	551	0.18	0.0560
(Cl^-)Etim-UiO-66	50	510	0.20	0.0490
FJI-C11	150	498	0.41	0.0119
(Cl^-)Etim-UiO-66	150	206	0.88	0.00628

Table S4. Adsorption capacities for dichromate on various MOFs.

MOF	The formula of MOFs	Maximum Capacities (mg/g)	Kinetic studies Equilibrium time at RT	Reference
ABT•2ClO_4	$[Ag_2\text{-}(btr)_2]\cdot 2ClO_4\cdot 3H_2O$	213-271	48h	4
FIR-53	$[Zn_2(Tipa)_2(OH)]\cdot 3NO_3\cdot 12H_2O$	74.2	10 min	5
FIR-54	$[Zn(Tipa)]\cdot 2NO_3\cdot DMF\cdot 4H_2O$	103	30 min	5
MOF-867		53.4	>12 h	6
ZJU-101		245	10 min	6
1-SO_4	$[\{Ni_2(L)_3\text{-}(SO_4)(H2O)_3\}\cdot(SO_4)\cdot x(G)]_n$	166	72 h	7
MOR-2	$H_{16}[Zr_6O_{16}(H_2PATP)_4]Cl_8\cdot xH_2O$	402.3	1 min	8
MOR-2-HA	MOR-2-alginic acid	338.1	1 min	8
1-Br	$[Cu_4(\mu_3\text{-}OH)_2(mtrb)_2(1,4\text{-}bda)_2]Br_2\cdot 6H_2O$	128	24-48 h	9
1-Cl	$\{Cu_2[CuCl(TTCA)(H_2O)_2]\}\cdot NO_3\cdot 4DMA\cdot 6H_2O$	65.8	180 min	10

1	$[Cu_2L(H_2O)_2]\cdot(NO_3)_2\cdot5.5H_2O$	222.5	91 min	11
$1\text{-}NO_3\text{-}OH\cdot20H_2O$	$[Cu_9(OH)_6Cl_2(itp)_6(1,4\text{-}bdc)_3](NO_3)_2(OH)_2\cdot20H_2O$	154.8	24-48 h	12
FJI-C11	$Cr_3(Cl/OH)(H_2O)_2O[(Cl^-)Etim\text{-}BDC]_3\cdot11H_2O$	321	3-5 min	This work

References

1. J. Liang, Y. Q. Xie, X. S. Wang, Q. Wang, T. T. Liu, Y. B. Huang and R. Cao, *Chem. Commun.*, 2018, **54**, 342-345.
2. Z. J. Lin, T. F. Liu, Y. B. Huang, J. Lu and R. Cao, *Chem. Eur. J.*, 2012, **18**, 7896-7902.
3. G. Ferey, C. Mellot-Draznieks, C. Serre, F. Millange, J. Dutour, S. Surble, I. Margiolaki, *Science*, 2005, **309**, 2040-2042.
4. X. Li, H. Xu, F. Kong and R. Wang, *Angew. Chem. Int. Ed. Engl.*, 2013, **52**, 13769-13773.
5. H.-R. Fu, Z.-X. Xu and J. Zhang, *Chem. Mater.*, 2014, **27**, 205-210.
6. Q. Zhang, J. Yu, J. Cai, L. Zhang, Y. Cui, Y. Yang, B. Chen and G. Qian, *Chem. Commun.*, 2015, **51**, 14732-14734.
7. AV. Desai, B. Manna, A. Karmakar, A. Sahu, SK. Ghosh, *Angew. Chem. Int. Ed. Engl.*, 2016, **55**, 7811-7815.
8. S. Rapti, D. Sarma, S. A. Diamantis, E. Skliri, G. S. Armatas, A. C. Tsipis, Y. S. Hassan, M. Alkordi, C. D. Malliakas, M. G. Kanatzidis, T. Lazarides, J. C. Plakatouras and M. J. Manos, *J. Mater. Chem. A*, 2017, **5**, 14707-14719.
9. X. X. Lv, L. L. Shi, K. Li, B. L. Li and H. Y. Li, *Chem. Commun.*, 2017, **53**, 1860-1863.
10. L. Ma, J. Yang, B. B. Lu, C. P. Li and J. F. Ma, *Inorg. Chem.*, 2018, **57**, 11746-11752.
11. C. Zhang, Y. Liu, L. Sun, H. Shi, C. Shi, Z. Liang and J. Li, *Chem. Eur. J.*, 2018, **24**, 2718-2724.
12. T. R. Zheng, L. L. Qian, M. Li, Z. X. Wang, K. Li, Y. Q. Zhang, B. L. Li and B. Wu, *Dalton Trans.*, 2018, **47**, 9103-9113.